Coherence Poincaré sphere of partially polarized optical beams

Jyrki Laatikainen,[1,*] Ari T. Friberg,[1] Olga Korotkova,[2] and Tero Setälä[1]
[1] *Institute of Photonics, University of Eastern Finland, P.O. Box 111, FI-80101 Joensuu, Finland*
[2] *Department of Physics, University of Miami, Coral Gables, Florida 33146, USA*

(Received 26 October 2021; accepted 23 February 2022; published 7 March 2022)

A Poincaré sphere representation of electromagnetic spectral two-point spatial coherence was recently introduced for fully polarized light beams. In this work, we employ the singular-value decomposition of the cross-spectral density matrix and establish a rigorous interpretation for the formalism in the context of partial polarization. At a single point, the construction reduces to the traditional polarization Poincaré sphere, which therefore can be regarded as a limiting case of the coherence sphere. The formalism is illustrated with paraxial blackbody radiation and Gaussian Schell-model beams. We expect our results will find use in understanding the coherence-polarization state of optical beams in situations dealing with random light.

DOI: 10.1103/PhysRevA.105.033506

I. INTRODUCTION

Spatial coherence is a fundamental characteristic of light fields which for scalar beams is traditionally quantified by the visibility of intensity fringes in Young's two-pinhole interference [1,2]. Today, it plays a vital role in diverse areas such as astronomy, interferometry, medical optics, and ghost imaging [3]. However, the recent progress in optical physics involving evanescent near fields and the growing complexity of components and systems in nanophotonics and plasmonics often call for rigorous electromagnetic treatment of light. Along with this development the electromagnetic theory of coherence with emphasis on the polarization features has attracted a great deal of research within the last two decades [4–9]. Among the very recent results is the introduction of the Poincaré sphere construction and the related Stokes parameters that graphically display the state of spatial electromagnetic coherence of fully polarized random light beams [10]. The paramount quantity was a matrix descriptor of two-point coherence whose mathematical properties are analogous to those of the conventional polarization matrix. The sphere representation of spatial coherence is similar to the customary Poincaré sphere in polarization optics [4] and the Bloch sphere of quantum mechanics [11].

In this paper, we establish the interpretation of the coherence Poincaré sphere for partially polarized light and show that for a general, nonuniformly partially polarized beam two coherence Poincaré vectors on the Poincaré sphere are needed which describe the state and degree of spatial coherence at two points. More precisely, the directions of the coherence vectors are determined by the singular vectors related to the larger singular value of the cross-spectral density matrix. When the two points coincide, the traditional polarization Poincaré sphere is obtained, whereas in the case of full polarization the results of [10] are found. The formalism is illustrated with paraxial radiation emanating from a blackbody cavity as well as with Gaussian Schell-model (GSM) beams.

The structure of this paper is as follows: in Sec. II we revisit the fundamental descriptors of electromagnetic coherence together with the matrix formalism that underlies the coherence Poincaré sphere. In Sec. III, the Poincaré sphere is introduced and interpreted for nonuniformly partially polarized beams. Section IV illustrates the formalism with examples. Finally, in Sec. V we briefly summarize the main findings of this work.

II. COHERENCE AND POLARIZATION OF ELECTROMAGNETIC BEAMS

A. Central concepts

We begin by recalling the concepts of electromagnetic coherence theory in the space-frequency domain that are relevant for this work. Our analysis considers a random, polychromatic, and statistically stationary electromagnetic beam whose electric-field realization at a point $\mathbf{r}$ and time t is given by $\mathbf{E}(\mathbf{r},t) = [E_x(\mathbf{r},t), E_y(\mathbf{r},t)]^{\mathrm{T}}$, with the superscript T denoting the matrix transpose. The spatial coherence properties of this beam are described by the 2×2 cross-spectral density (CSD) matrix [2,4,7,12]

$$\mathbf{W}(\mathbf{r}_1,\mathbf{r}_2) = \frac{1}{2\pi}\int_{-\infty}^{\infty} \mathbf{\Gamma}(\mathbf{r}_1,\mathbf{r}_2,\tau)e^{i\omega\tau}d\tau = \begin{bmatrix} W_{xx}(\mathbf{r}_1,\mathbf{r}_2) & W_{xy}(\mathbf{r}_1,\mathbf{r}_2) \\ W_{yx}(\mathbf{r}_1,\mathbf{r}_2) & W_{yy}(\mathbf{r}_1,\mathbf{r}_2) \end{bmatrix}, \tag{1}$$

which is obtained via the Wiener-Khintchine theorem as the Fourier transform of the mutual coherence matrix $\mathbf{\Gamma}(\mathbf{r}_1,\mathbf{r}_2,\tau) = \langle \mathbf{E}^*(\mathbf{r}_1,t)\mathbf{E}^{\mathrm{T}}(\mathbf{r}_2,t+\tau)\rangle$. In these expressions $\tau = t_2 - t_1$, and the angle brackets and asterisk stand for the time average and complex conjugate, respectively. If the field is ergodic, the brackets may also denote ensemble averaging. For brevity, here and henceforth, the frequency dependence is not explicitly shown in the spectral quantities. The polarization properties of the field are specified by the polarization

*Corresponding author: jyrki.laatikainen@uef.fi

matrix defined by $\mathbf{\Phi}(\mathbf{r}) = \mathbf{W}(\mathbf{r}, \mathbf{r})$. The polarization matrix is Hermitian, $\mathbf{\Phi}(\mathbf{r}) = \mathbf{\Phi}^{\dagger}(\mathbf{r})$, with the dagger denoting the Hermitian adjoint, whereas the CSD matrix is quasi-Hermitian in the sense that $\mathbf{W}^{\dagger}(\mathbf{r}_1, \mathbf{r}_2) = \mathbf{W}(\mathbf{r}_2, \mathbf{r}_1)$. Both matrices satisfy certain non-negative definiteness conditions [2]. Furthermore, the polarization matrix of any light beam can be uniquely expressed as the sum

$$\mathbf{\Phi}(\mathbf{r}) = \mathbf{\Phi}^{(\mathrm{u})}(\mathbf{r}) + \mathbf{\Phi}^{(\mathrm{p})}(\mathbf{r}), \tag{2}$$

where the former matrix represents a completely unpolarized field and the latter represents a fully polarized field. The degree of polarization is then defined as [2,4,7]

$$P(\mathbf{r}) = \frac{\mathrm{tr}\,\mathbf{\Phi}^{(\mathrm{p})}(\mathbf{r})}{\mathrm{tr}\,\mathbf{\Phi}(\mathbf{r})} = \left[1 - \frac{4\det\mathbf{\Phi}(\mathbf{r})}{\mathrm{tr}^2\mathbf{\Phi}(\mathbf{r})}\right]^{1/2}, \tag{3}$$

with det and tr denoting the matrix determinant and trace, respectively. Physically, this quantity therefore describes the spectral density ratio of the polarized part and the total beam. The degree of polarization is bounded as $0 \leqslant P(\mathbf{r}) \leqslant 1$, where the lower and upper limits correspond to unpolarized and fully polarized fields, respectively [2].

Another frequently used representation for the polarization of light is the set of one-point Stokes parameters that can be written in terms of the polarization matrix elements $\Phi_{\alpha\beta}(\mathbf{r}) = W_{\alpha\beta}(\mathbf{r}, \mathbf{r})$, with $(\alpha, \beta) \in (x, y)$, as [4]

$$S_0(\mathbf{r}) = \Phi_{xx}(\mathbf{r}) + \Phi_{yy}(\mathbf{r}), \tag{4a}$$
$$S_1(\mathbf{r}) = \Phi_{xx}(\mathbf{r}) - \Phi_{yy}(\mathbf{r}), \tag{4b}$$
$$S_2(\mathbf{r}) = \Phi_{xy}(\mathbf{r}) + \Phi_{yx}(\mathbf{r}), \tag{4c}$$
$$S_3(\mathbf{r}) = i[\Phi_{yx}(\mathbf{r}) - \Phi_{xy}(\mathbf{r})]. \tag{4d}$$

These parameters are real and can be normalized via $s_j(\mathbf{r}) = S_j(\mathbf{r})/S_0(\mathbf{r})$, $j \in (0, \ldots, 3)$. Their illustrative value is manifested with the renowned construction of the polarization Poincaré sphere that includes all possible states of polarization, full or partial, as points on or within a unit sphere in (s_1, s_2, s_3) space. This representation is based on the expression

$$s_1^2(\mathbf{r}) + s_2^2(\mathbf{r}) + s_3^2(\mathbf{r}) = P^2(\mathbf{r}), \tag{5}$$

and the corresponding Poincaré vector is defined as $\mathbf{s}(\mathbf{r}) = [s_1(\mathbf{r}), s_2(\mathbf{r}), s_3(\mathbf{r})]$. The length of the Poincaré vector is thus given by the degree of polarization $|\mathbf{s}(\mathbf{r})| = P(\mathbf{r})$, while the direction is determined by the state of polarization related to $\mathbf{\Phi}^{(\mathrm{p})}(\mathbf{r})$ in Eq. (2).

The electromagnetic degree of coherence that indicates the level of two-point correlations between the electric field components is defined (in squared form) as [9,13]

$$\mu^2(\mathbf{r}_1, \mathbf{r}_2) = \frac{\mathrm{tr}[\mathbf{W}^{\dagger}(\mathbf{r}_1, \mathbf{r}_2)\mathbf{W}(\mathbf{r}_1, \mathbf{r}_2)]}{S_0(\mathbf{r}_1)S_0(\mathbf{r}_2)}. \tag{6}$$

The physical interpretation of this quantity relates to the sum of contrasts of the spectral density and polarization-state modulations in interference [14]. It is normalized as $0 \leqslant \mu(\mathbf{r}_1, \mathbf{r}_2) \leqslant 1$, with the lower and upper bounds representing complete incoherence and full coherence, respectively, at the two points on frequency ω.

B. The Gram matrix representation of electromagnetic spatial coherence

We proceed to consider the coherence information contained in the matrix

$$\mathbf{\Omega}(\mathbf{r}_1, \mathbf{r}_2) = \mathbf{W}^{\dagger}(\mathbf{r}_1, \mathbf{r}_2)\mathbf{W}(\mathbf{r}_1, \mathbf{r}_2) \tag{7}$$

and introduce the abbreviations $\mathbf{W}(\mathbf{r}_1, \mathbf{r}_2) = \mathbf{W}_{12}$ and $\mathbf{\Omega}(\mathbf{r}_1, \mathbf{r}_2) = \mathbf{\Omega}_{12}$, which will be employed throughout the text for legibility unless clarity requires otherwise. The matrix $\mathbf{\Omega}_{12}$ is formally defined as the Gram matrix [15] of the set of CSD matrix columns, and it is by definition a Hermitian and non-negative-definite matrix obeying $\mathbf{\Omega}_{12}^{\dagger} = \mathbf{\Omega}_{12}$ and $\det\mathbf{\Omega}_{12} \geqslant 0$. These are the key mathematical properties that $\mathbf{\Omega}_{12}$ shares with the traditional polarization matrix, and they constitute the main motivation for the description of coherence in terms of $\mathbf{\Omega}_{12}$.

We note that the unique decomposition [10]

$$\mathbf{\Omega}_{12} = \mathbf{\Omega}_{12}^{(\mathrm{u})} + \mathbf{\Omega}_{12}^{(\mathrm{p})} = A_{12}\begin{bmatrix}1 & 0\\ 0 & 1\end{bmatrix} + \begin{bmatrix}B_{12} & D_{12}\\ D_{12}^{*} & C_{12}\end{bmatrix}, \tag{8}$$

with $A_{12}, B_{12}, C_{12} \geqslant 0$ and $\det\mathbf{\Omega}_{12}^{(\mathrm{p})} = 0$, holds for any pair of points. This feature is analogous to the decomposition of the polarization matrix into the parts corresponding to an unpolarized beam and a polarized beam in Eq. (2). Introducing notation for the elements of $\mathbf{\Omega}_{12}$ via

$$\mathbf{\Omega}_{12} = \begin{bmatrix}\Omega_{xx}(\mathbf{r}_1, \mathbf{r}_2) & \Omega_{xy}(\mathbf{r}_1, \mathbf{r}_2)\\ \Omega_{yx}(\mathbf{r}_1, \mathbf{r}_2) & \Omega_{yy}(\mathbf{r}_1, \mathbf{r}_2)\end{bmatrix}, \tag{9}$$

the parameters A_{12}, B_{12}, C_{12}, and D_{12} can be equivalently written in terms of the $\mathbf{\Omega}_{12}$ elements as

$$A_{12} = \frac{1}{2}\mathrm{tr}\,\mathbf{\Omega}_{12} - \frac{1}{2}\sqrt{\mathrm{tr}^2\,\mathbf{\Omega}_{12} - 4\det\mathbf{\Omega}_{12}}, \tag{10a}$$

$$B_{12} = \frac{1}{2}[\Omega_{xx}(\mathbf{r}_1, \mathbf{r}_2) - \Omega_{yy}(\mathbf{r}_1, \mathbf{r}_2)] + \frac{1}{2}\sqrt{\mathrm{tr}^2\,\mathbf{\Omega}_{12} - 4\det\mathbf{\Omega}_{12}}, \tag{10b}$$

$$C_{12} = \frac{1}{2}[\Omega_{yy}(\mathbf{r}_1, \mathbf{r}_2) - \Omega_{xx}(\mathbf{r}_1, \mathbf{r}_2)] + \frac{1}{2}\sqrt{\mathrm{tr}^2\,\mathbf{\Omega}_{12} - 4\det\mathbf{\Omega}_{12}}, \tag{10c}$$

$$D_{12} = \Omega_{xy}(\mathbf{r}_1, \mathbf{r}_2). \tag{10d}$$

However, unlike with the polarization matrix, in the context of $\mathbf{\Omega}_{12}$ the total field is not an incoherent mixture of the two fields corresponding to $\mathbf{\Omega}_{12}^{(\mathrm{u})}$ and $\mathbf{\Omega}_{12}^{(\mathrm{p})}$. Further, the related matrices $\mathbf{W}_{12}^{(\mathrm{u})}$ and $\mathbf{W}_{12}^{(\mathrm{p})}$ and fields are not unique.

We emphasize that in general $\mathbf{\Omega}_{12} \neq \mathbf{\Omega}_{21}$, and thus, the coherence information in the two matrices is different. However, it is presumable that these matrices are connected according to the quasi-Hermiticity of the CSD matrix. Insight into this feature is gained by invoking the singular-value decomposition (SVD) [16] of the CSD. The SVD reads $\mathbf{W}_{12} = \mathbf{U}\mathbf{D}\mathbf{V}^{\dagger}$, where $\mathbf{U} = [\hat{\mathbf{u}}_+, \hat{\mathbf{u}}_-]$ and $\mathbf{V} = [\hat{\mathbf{v}}_+, \hat{\mathbf{v}}_-]$ are unitary matrices and $\mathbf{D} = \mathrm{diag}[\nu_+, \nu_-]$, with ν_+ and ν_- being the singular values of the CSD. The columns of $\mathbf{U}$ and $\mathbf{V}$ are complex unit vectors obeying $\mathbf{W}_{12}\hat{\mathbf{v}}_{\pm} = \nu_{\pm}\hat{\mathbf{u}}_{\pm}$ and $\mathbf{W}_{12}^{\dagger}\hat{\mathbf{u}}_{\pm} = \nu_{\pm}\hat{\mathbf{v}}_{\pm}$. The singular values are real and satisfy $\nu_+ \geqslant \nu_- \geqslant 0$. It readily follows that

$\hat{\mathbf{v}}_\pm$ and $\hat{\mathbf{u}}_\pm$ are the eigenvectors of $\mathbf{\Omega}_{12}$ and $\mathbf{\Omega}_{21}$, respectively, while $\nu_\pm^2$ are the related eigenvalues for both matrices, i.e., $\mathbf{\Omega}_{12}\hat{\mathbf{v}}_\pm = \nu_\pm^2\hat{\mathbf{v}}_\pm$ and $\mathbf{\Omega}_{21}\hat{\mathbf{u}}_\pm = \nu_\pm^2\hat{\mathbf{u}}_\pm$. These eigenvalue equations admit analytical solutions leading to the singular values of the form (see, e.g., [8,16,17])

$$\nu_\pm^2 = \tfrac{1}{2}\mathrm{tr}\,\mathbf{\Omega}_{12}[1 \pm P_\Omega(\mathbf{r}_1, \mathbf{r}_2)], \tag{11}$$

where

$$P_\Omega(\mathbf{r}_1, \mathbf{r}_2) = \frac{\mathrm{tr}\,\mathbf{\Omega}_{12}^{(\mathrm{p})}}{\mathrm{tr}\,\mathbf{\Omega}_{12}} = \left(1 - \frac{4\det\mathbf{\Omega}_{12}}{\mathrm{tr}^2\mathbf{\Omega}_{12}}\right)^{1/2} \tag{12}$$

satisfies $0 \leqslant P_\Omega(\mathbf{r}_1, \mathbf{r}_2) \leqslant 1$ and can be viewed as representing the (trace) portion of $\mathbf{\Omega}_{12}^{(\mathrm{p})}$ in $\mathbf{\Omega}_{12}$. The definition of P_Ω is analogous to that of P in Eq. (3) but in the context of $\mathbf{\Omega}_{12}$. Furthermore, we can write

$$\mathbf{\Omega}_{12} = \nu_+^2\hat{\mathbf{v}}_+\hat{\mathbf{v}}_+^\dagger + \nu_-^2\hat{\mathbf{v}}_-\hat{\mathbf{v}}_-^\dagger, \tag{13}$$

$$\mathbf{\Omega}_{21} = \nu_+^2\hat{\mathbf{u}}_+\hat{\mathbf{u}}_+^\dagger + \nu_-^2\hat{\mathbf{u}}_-\hat{\mathbf{u}}_-^\dagger. \tag{14}$$

We have thus established the connection of $\mathbf{\Omega}_{12}$ and $\mathbf{\Omega}_{21}$ via the SVD of the CSD matrix. The interpretation of these expressions will be developed further in Sec. III.

We shall illustrate the implications of the cases $P_\Omega = 1$ and $P_\Omega = 0$, which are of specific interest as the bounds of P_Ω. To this aim we employ Eq. (11) and write

$$P_\Omega(\mathbf{r}_1, \mathbf{r}_2) = \frac{\nu_+^2 - \nu_-^2}{\nu_+^2 + \nu_-^2}. \tag{15}$$

The condition $P_\Omega = 1$ is equivalent to $\nu_- = 0$ and the CSD matrix being singular. It then factorizes due to the SVD as $\mathbf{W}_{12} = \nu_+\hat{\mathbf{u}}_+\hat{\mathbf{v}}_+^\dagger$, leading to $\mathbf{\Omega}_{12} = \nu_+^2\hat{\mathbf{v}}_+\hat{\mathbf{v}}_+^\dagger$. For $\mathbf{W}_{21}$ we find $\mathbf{W}_{21} = \nu_+\hat{\mathbf{v}}_+\hat{\mathbf{u}}_+^\dagger$, resulting in $\mathbf{\Omega}_{21} = \nu_+^2\hat{\mathbf{u}}_+\hat{\mathbf{u}}_+^\dagger$. When $P_\Omega = 1$ holds everywhere, then $\mathbf{\Omega}_{12} = \mathbf{\Omega}_{12}^{(\mathrm{p})}$ in Eq. (8), and the field is necessarily fully polarized at all points [10]. This point allows us to connect the SVD to the coherence characteristics. Indeed, it was shown earlier (see the supplement in [10]) that for a nonuniformly fully polarized beam the CSD can be written as $\mathbf{W}_{12} = W_{12}\hat{\mathbf{a}}_1^*\hat{\mathbf{a}}_2^{\mathrm{T}}$, where W_{12} is a scalar-field CSD function and the complex (column) unit vector $\hat{\mathbf{a}}_j$ represents the normalized Jones vector at point $\mathbf{r}_j$, $j \in (1, 2)$. It follows that

$$\mathbf{\Omega}_{12} = |W_{12}|^2\hat{\mathbf{a}}_2^*\hat{\mathbf{a}}_2^{\mathrm{T}}. \tag{16}$$

In an analogous manner we would find that $\mathbf{\Omega}_{21} = |W_{12}|^2\hat{\mathbf{a}}_1^*\hat{\mathbf{a}}_1^{\mathrm{T}}$. It is now evident that $\nu_+ = |W_{12}|$, $\hat{\mathbf{v}}_+ = \hat{\mathbf{a}}_2^*$, and $\hat{\mathbf{u}}_+ = \hat{\mathbf{a}}_1^*$. As a summary, we see that $\mathbf{\Omega}_{12}$ expresses the polarization state in $\mathbf{r}_2$, while $\mathbf{\Omega}_{21}$ does so in $\mathbf{r}_1$. These results highlight, in view of the SVD and the Jones vectors, the different information content of $\mathbf{\Omega}_{12}$ and $\mathbf{\Omega}_{21}$ in the case of $P_\Omega = 1$.

If $P_\Omega = 0$ holds, Eq. (15) implies that the CSD matrix has a degenerate singular value $\nu = \nu_+ = \nu_-$. According to the SVD, the CSD matrix is generally of the form $\mathbf{W}_{12} = \nu\mathbf{M}_{12}$, where $\mathbf{M}_{12} = \mathbf{U}\mathbf{V}^\dagger$ is a unitary matrix. In this special case the CSD matrix is normal, $\mathbf{W}_{12}^\dagger\mathbf{W}_{12} = \mathbf{W}_{12}\mathbf{W}_{12}^\dagger$, and thus, $\mathbf{\Omega}_{12} = \mathbf{\Omega}_{21}$. In other words, the information contents of the two matrices are the same. Moreover, if $P_\Omega = 0$ holds throughout the considered volume, the field is necessarily unpolarized in that domain [10]. However, we remark that not all unpolarized fields obey this condition. Specific examples of fields with $P_\Omega = 0$ are the pure unpolarized states that remain unpolarized in Young's interferometer [18]. Their CSD matrix is of the form $\mathbf{W}_{12} = W_{12}\mathbf{I}$, where $\mathbf{I}$ is the 2×2 identity matrix. Consequently, for every $\mathbf{\Omega}_{12}^{(\mathrm{u})}$ one can associate $\mathbf{W}_{12}$ of a pure unpolarized beam, although the CSD matrix does not have to be of this form since in general $\mathbf{W}_{12} = \nu\mathbf{M}_{12}$. However, this general expression can be rendered in the form of a pure unpolarized beam using the operations $\mathbf{U}^\dagger\mathbf{W}_{12}\mathbf{V}$. In other words, every field with $P_\Omega = 0$ can be formally transformed into a pure unpolarized beam by performing the unitary operations $\mathbf{U}^*$ at $\mathbf{r}_1$ and $\mathbf{V}^{\mathrm{T}}$ at $\mathbf{r}_2$.

III. COHERENCE POINCARÉ SPHERE

In this section, we illustrate the content of matrix $\mathbf{\Omega}_{12}$ at two points in terms of the geometrical representation that we call the coherence Poincaré sphere [10]. Next, we establish a rigorous interpretation of the coherence Poincaré sphere for all electromagnetic beams regardless of the state and degree of polarization.

The Hermiticity of $\mathbf{\Omega}_{12}$ allows us to form four real-valued Stokes parameters analogous to those of the polarization matrix listed in Eqs. (4a)–(4d) [10]. The related Stokes parameters are given in terms of Eq. (9) as

$$Q_0(\mathbf{r}_1, \mathbf{r}_2) = \Omega_{xx}(\mathbf{r}_1, \mathbf{r}_2) + \Omega_{yy}(\mathbf{r}_1, \mathbf{r}_2), \tag{17a}$$

$$Q_1(\mathbf{r}_1, \mathbf{r}_2) = \Omega_{xx}(\mathbf{r}_1, \mathbf{r}_2) - \Omega_{yy}(\mathbf{r}_1, \mathbf{r}_2), \tag{17b}$$

$$Q_2(\mathbf{r}_1, \mathbf{r}_2) = \Omega_{xy}(\mathbf{r}_1, \mathbf{r}_2) + \Omega_{yx}(\mathbf{r}_1, \mathbf{r}_2), \tag{17c}$$

$$Q_3(\mathbf{r}_1, \mathbf{r}_2) = i[\Omega_{yx}(\mathbf{r}_1, \mathbf{r}_2) - \Omega_{xy}(\mathbf{r}_1, \mathbf{r}_2)]. \tag{17d}$$

These quantities can be written at two points or in a single point, and they can be normalized with the spectral density via

$$q_j(\mathbf{r}_1, \mathbf{r}_2) = \frac{Q_j(\mathbf{r}_1, \mathbf{r}_2)}{S_0(\mathbf{r}_1)S_0(\mathbf{r}_2)}, \quad j \in (0, \ldots, 3). \tag{18}$$

The Poincaré sphere of electromagnetic spatial coherence for a general partially polarized beam is then defined by the equation

$$q_1^2(\mathbf{r}_1, \mathbf{r}_2) + q_2^2(\mathbf{r}_1, \mathbf{r}_2) + q_3^2(\mathbf{r}_1, \mathbf{r}_2) = P_\Omega^2(\mathbf{r}_1, \mathbf{r}_2)\mu^4(\mathbf{r}_1, \mathbf{r}_2), \tag{19}$$

with μ and P_Ω given in Eqs. (6) and (12), respectively. The above relation forms an origin-centered sphere with a radius of $0 \leqslant P_\Omega\mu^2 \leqslant 1$ in (q_1, q_2, q_3) space. This sphere together with the coherence Poincaré vector

$$\mathbf{q}(\mathbf{r}_1, \mathbf{r}_2) = [q_1(\mathbf{r}_1, \mathbf{r}_2), q_2(\mathbf{r}_1, \mathbf{r}_2), q_3(\mathbf{r}_1, \mathbf{r}_2)] \tag{20}$$

provides a graphical representation for electromagnetic spatial coherence. The length of $\mathbf{q}$ is $P_\Omega\mu^2$, and its direction describes the state of electromagnetic spatial coherence of the beam, as will be illustrated shortly. First, we inspect spatially fully coherent beams with $\mu = 1$. This necessitates that $P_\Omega = 1$ [10], and we see that the surface of the sphere, $|\mathbf{q}| = 1$, corresponds to complete spatial coherence. Second, the origin encompasses the cases of $\mu = 0$ and/or $P_\Omega = 0$. The former condition exclusively implies complete spatial incoherence, while the latter includes the pure unpolarized beams and those which can be transformed to that type by the specific unitary operations at the two points, as discussed earlier.

Next, we interpret the direction of the coherence Poincaré vector $\mathbf{q}_{12} = \mathbf{q}(\mathbf{r}_1, \mathbf{r}_2)$. Equation (8) and the properties $B_{12} \geqslant 0$, $C_{12} \geqslant 0$, and $\det \mathbf{\Omega}_{12}^{(\mathrm{p})} = 0$ allow us to decompose $\mathbf{\Omega}_{12}^{(\mathrm{p})}$ into the form

$$\mathbf{\Omega}_{12}^{(\mathrm{p})} = \operatorname{tr} \mathbf{\Omega}_{12}^{(\mathrm{p})} \hat{\mathbf{e}}_{12}^{*} \hat{\mathbf{e}}_{12}^{\mathrm{T}}, \tag{21}$$

where $\hat{\mathbf{e}}_{12} = [e_{12x}, e_{12y}]^{\mathrm{T}}$ is a complex unit vector describing the beam's state of electromagnetic spatial coherence at points $\mathbf{r}_1$ and $\mathbf{r}_2$. Comparison of Eqs. (8) and (21) yields $|e_{12x}| = \sqrt{B_{12}/(B_{12}+C_{12})}$, $|e_{12y}| = \sqrt{C_{12}/(B_{12}+C_{12})}$, and $D_{12} = \sqrt{B_{12}C_{12}} \exp[i(\varphi_{12y} - \varphi_{12x})]$, with φ_{12x} and φ_{12y} denoting the phases of e_{12x} and e_{12y}, respectively. Inserting Eq. (21) into Eq. (8) and then using Eqs. (10a) and (12) result in

$$\mathbf{\Omega}_{12} = \operatorname{tr} \mathbf{\Omega}_{12} \left(\frac{1 - P_\Omega}{2} \mathbf{I} + P_\Omega \hat{\mathbf{e}}_{12}^{*} \hat{\mathbf{e}}_{12}^{\mathrm{T}} \right). \tag{22}$$

It is insightful to contrast this representation with the implications of the SVD of CSD. Equations (13) and (11), together with the fact that $\hat{\mathbf{v}}_+ \hat{\mathbf{v}}_+^\dagger + \hat{\mathbf{v}}_- \hat{\mathbf{v}}_-^\dagger = \mathbf{I}$, lead to

$$\mathbf{\Omega}_{12} = \operatorname{tr} \mathbf{\Omega}_{12} \left(\frac{1 - P_\Omega}{2} \mathbf{I} + P_\Omega \hat{\mathbf{v}}_+ \hat{\mathbf{v}}_+^\dagger \right), \tag{23}$$

and thus, $\hat{\mathbf{e}}_{12} = \hat{\mathbf{v}}_+^*$. An analogous consideration for $\mathbf{\Omega}_{21}$ shows that $\hat{\mathbf{e}}_{21} = \hat{\mathbf{u}}_+^*$. The vectors $\hat{\mathbf{e}}_{12}$ and $\hat{\mathbf{e}}_{21}$ therefore directly describe the complex conjugates of the singular vectors pertaining to the larger singular value of the CSD.

Using Eq. (22), the $\mathbf{\Omega}_{12}$ matrix Stokes parameters take the forms

$$Q_0(\mathbf{r}_1, \mathbf{r}_2) = 2A_{12} + \operatorname{tr} \mathbf{\Omega}_{12}^{(\mathrm{p})}, \tag{24a}$$

$$Q_1(\mathbf{r}_1, \mathbf{r}_2) = \operatorname{tr} \mathbf{\Omega}_{12}^{(\mathrm{p})} (|e_{12x}|^2 - |e_{12y}|^2), \tag{24b}$$

$$Q_2(\mathbf{r}_1, \mathbf{r}_2) = \operatorname{tr} \mathbf{\Omega}_{12}^{(\mathrm{p})} 2\mathrm{Re}(e_{12x}^* e_{12y}), \tag{24c}$$

$$Q_3(\mathbf{r}_1, \mathbf{r}_2) = \operatorname{tr} \mathbf{\Omega}_{12}^{(\mathrm{p})} 2\mathrm{Im}(e_{12x}^* e_{12y}), \tag{24d}$$

where Re and Im denote the real and imaginary parts, respectively. We may normalize these quantities via Eq. (18), make use of Eq. (6) together with Eq. (12), and after straightforward developments find that

$$\mathbf{q}_{12} = P_\Omega \mu^2 \hat{\mathbf{s}}_{12}, \tag{25}$$

where

$$\hat{\mathbf{s}}_{12} = [|e_{12x}|^2 - |e_{12y}|^2, 2\mathrm{Re}(e_{12x}^* e_{12y}), 2\mathrm{Im}(e_{12x}^* e_{12y})] \tag{26}$$

is the unit-length vector specified by $\hat{\mathbf{e}}_{12}$ and determines the direction of $\mathbf{q}_{12}$. Using an analogous procedure, we see that $\mathbf{q}_{21} = \mathbf{q}(\mathbf{r}_2, \mathbf{r}_1)$ can be expressed as

$$\mathbf{q}_{21} = P_\Omega \mu^2 \hat{\mathbf{s}}_{21}, \tag{27}$$

where $\hat{\mathbf{s}}_{21}$ is defined in analogy to Eq. (26), but for $\hat{\mathbf{e}}_{21}$. We conclude that for every matrix $\mathbf{\Omega}_{12}$ with $P_\Omega \neq 0$ there is a vector $\hat{\mathbf{e}}_{12} = \mathbf{v}_+^*$ which unambiguously determines the direction of $\mathbf{q}_{12}$. Further, the direction of $\mathbf{q}_{21}$ that characterizes $\mathbf{\Omega}_{21}$ is exclusively determined by $\hat{\mathbf{e}}_{21} = \mathbf{u}_+^*$. The two coherence vectors are separated by the central angle

$$\theta_{12} = \arccos(\hat{\mathbf{s}}_{12} \cdot \hat{\mathbf{s}}_{21}), \tag{28}$$

which is bounded as $0 \leqslant \theta_{12} \leqslant \pi$. This angle is a geometric measure of similarity between the electromagnetic coherence states at the two points described by $\mathbf{q}_{12}$ and $\mathbf{q}_{21}$. The lower bound $\theta_{12} = 0$ is obtained when $\mathbf{q}_{12} = \mathbf{q}_{21}$. The upper limit $\theta_{12} = \pi$ indicates that the vectors are inverse, $\mathbf{q}_{12} = -\mathbf{q}_{21}$.

The single-point version of vector $\hat{\mathbf{e}}_{12}$ reduces to the complex unit (Jones) vector that represents the state of polarization at that point, as is shown next. To this aim we select, say, point $\mathbf{r}_1$ and notice that the singular values $\nu_\pm$ of the polarization matrix $\mathbf{\Phi}_1$ coincide with its eigenvalues [16]. Likewise, the corresponding singular vectors $\hat{\mathbf{v}}_\pm = \hat{\mathbf{u}}_\pm$ are the eigenvectors of this matrix. Moreover, since Eqs. (22) and (23) hold also at a single point, we confirm that $\hat{\mathbf{e}}_{11} = \hat{\mathbf{v}}_+^*$. Consequently, $\hat{\mathbf{e}}_{11}^*$ is the eigenvector associated with the larger eigenvalue of the polarization matrix. We then utilize the decomposition $\mathbf{\Phi}_1 = \nu_+ \hat{\mathbf{v}}_+ \hat{\mathbf{v}}_+^\dagger + \nu_- \hat{\mathbf{v}}_- \hat{\mathbf{v}}_-^\dagger$. Using Eq. (3) together with the orthonormality of $\hat{\mathbf{v}}_+$ and $\hat{\mathbf{v}}_-$, this decomposition is expressible in the form

$$\mathbf{\Phi}_1 = \operatorname{tr} \mathbf{\Phi}_1 \left(\frac{1 - P}{2} \mathbf{I} + P \hat{\mathbf{v}}_+ \hat{\mathbf{v}}_+^\dagger \right). \tag{29}$$

We also revisit Eq. (2) and note that the single-point form of the CSD matrix for the polarized constituent (Sec. II B) can be written as $\mathbf{\Phi}_1^{(\mathrm{p})} = \operatorname{tr} \mathbf{\Phi}_1^{(\mathrm{p})} \hat{\mathbf{a}}_1^* \hat{\mathbf{a}}_1^{\mathrm{T}}$. This together with Eq. (3) and the formal analogy of Eq. (10a) allow us to express Eq. (2) in the form

$$\mathbf{\Phi}_1 = \operatorname{tr} \mathbf{\Phi}_1 \left(\frac{1 - P}{2} \mathbf{I} + P \hat{\mathbf{a}}_1^* \hat{\mathbf{a}}_1^{\mathrm{T}} \right). \tag{30}$$

A comparison of Eqs. (29) and (30) shows that $\hat{\mathbf{v}}_+ = \hat{\mathbf{a}}_1^*$. Therefore, $\hat{\mathbf{e}}_{11}$ equals the Jones vector $\hat{\mathbf{a}}_1$ representing the polarization state of the polarized constituent at $\mathbf{r}_1$. Consequently, the corresponding single-point unit vector $\hat{\mathbf{s}}_{11}$ on the coherence Poincaré sphere reduces to the traditional polarization Poincaré vector $\mathbf{s}_1$. Naturally, analogous reductions hold at $\mathbf{r}_2$.

We summarize the relevant properties of the coherence Poincaré vectors $\mathbf{q}_{12}$ and $\mathbf{q}_{21}$, which are illustrated in Fig. 1 in (q_1, q_2, q_3) space. Their lengths are the same and equal to $P_\Omega \mu^2$, where both P_Ω and μ are invariant under the interchange of $\mathbf{r}_1$ and $\mathbf{r}_2$. Hence, the tips of $\mathbf{q}_{12}$ and $\mathbf{q}_{21}$ are on the same sphere in (q_1, q_2, q_3) space, and their separation is quantified by the central angle θ_{12} in Eq. (28). Equations (25) and (27) constitute the interpretation of the coherence Poincaré sphere in the context of partially polarized light beams, where $\hat{\mathbf{s}}_{12}$ and $\hat{\mathbf{s}}_{21}$ are determined by $\hat{\mathbf{v}}_+^*$ and $\hat{\mathbf{u}}_+^*$, respectively, i.e., the (conjugates of) singular vectors corresponding to the larger singular value of the CSD. If the field is fully polarized throughout [10], $P_\Omega = 1$ is valid, and $\mathbf{q}_{12} = \mu^2 \mathbf{s}_2$, and $\mathbf{q}_{21} = \mu^2 \mathbf{s}_1$, where the length is defined by the degree of coherence μ alone and the polarization Poincaré vectors $\mathbf{s}_2$ and $\mathbf{s}_1$ at the indicated points specify the directions. This shows that the axes of the coherence Poincaré space represent the polarization state in full analogy to the single-point formalism. Thus, x and y polarized beams are located on the q_1 axis; $\pm 45^\circ$ polarized beams are on the q_2 axis, and the right-handed and left-handed circularly polarized beams are on the q_3 axis, in the case of

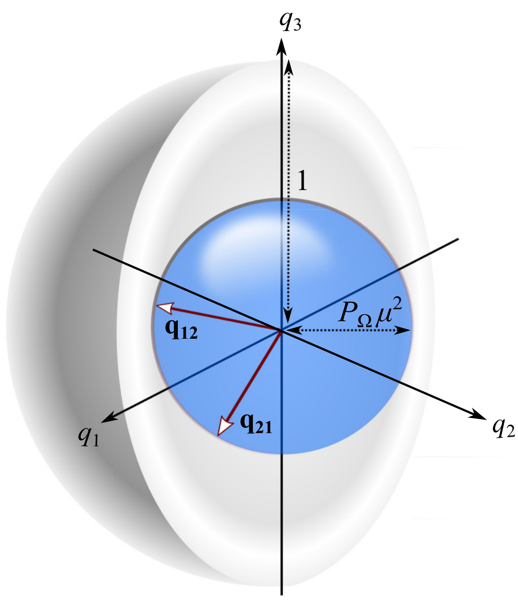

FIG. 1. Illustration of the coherence Poincaré sphere that displays the state of two-point electromagnetic coherence of a random, generally partially polarized light beam. The distance from the origin is $P_\Omega\mu^2$, and the directions of vectors $\mathbf{q}_{12}$ and $\mathbf{q}_{21}$ are specified by the state of spatial coherence at points $\mathbf{r}_1$ and $\mathbf{r}_2$.

complete polarization. Both vectors are needed to illustrate the coherence-polarization information of a nonuniformly fully polarized beam on the sphere. If the beam is uniformly polarized, then $\mathbf{s}_1 = \mathbf{s}_2 = \mathbf{s}$, and only a single vector $\mathbf{q} = \mu^2\mathbf{s}$ is required [10]. Finally, in a single point, regardless of the degree of polarization, $\mathbf{q} = P^2\mathbf{s}$ is true [10], showing that the traditional Poincaré sphere is a limiting case of the Poincaré sphere of two-point spatial coherence, and in the present context it can be interpreted as a geometrical representation of the single-point coherence properties of electromagnetic beams.

IV. EXAMPLES

A. Blackbody radiation

As the first example we consider the radiation emanating from a circular opening in a cavity containing blackbody radiation. The 2×2 CSD matrix of the paraxial far field at a distance of r in the directions specified by the unit vectors $\hat{\mathbf{r}}_1$ and $\hat{\mathbf{r}}_2$ can be expressed as [19,20]

$$\mathbf{W}(r\hat{\mathbf{r}}_1, r\hat{\mathbf{r}}_2) = \frac{2\mathcal{A}a_0(\omega)}{r^2}\frac{J_1(k\epsilon\varrho)}{k\epsilon\varrho}\mathbf{I}. \tag{31}$$

Above, $\mathcal{A} = \pi\epsilon^2$ is the area of the aperture with radius ϵ, $J_1(x)$ is the first-order Bessel function, and $k = 2\pi/\lambda$ is the free-space wave number corresponding to wavelength λ. In addition, $\varrho = |\boldsymbol{\varrho}_2 - \boldsymbol{\varrho}_1|$, with $\boldsymbol{\varrho}_j$ being the projection of $\hat{\mathbf{r}}_j$, $j \in (1, 2)$, onto the aperture plane, and $a_0(\omega)$ is the Planck spectrum as defined in [20]. The CSD matrix and the related $\boldsymbol{\Omega}_{12}$ are both proportional to the identity matrix conforming to a pure unpolarized beam. Consequently, the normalized Stokes parameters of $\boldsymbol{\Omega}_{12}$ are

$$q_0 = 2\left[\frac{J_1(k\epsilon\varrho)}{k\epsilon\varrho}\right]^2 = \mu^2, \tag{32a}$$

$$q_1 = q_2 = q_3 = 0, \tag{32b}$$

and hence, the coherence Poincaré vector is $\mathbf{q} = (0, 0, 0)$. Further, $P_\Omega = 0$ holds. In conclusion, the paraxial far field of a blackbody cavity is positioned in the origin of the Stokes parameter space.

B. Gaussian Schell-model beams

Consider an electromagnetic GSM beam for which the elements of the CSD matrix at the waist are generally expressed as [7]

$$W_{\alpha\beta}(\mathbf{r}_1, \mathbf{r}_2, \omega) = A_\alpha A_\beta B_{\alpha\beta}\exp\left[-\left(\frac{\mathbf{r}_1^2}{2\sigma_\alpha^2} + \frac{\mathbf{r}_2^2}{2\sigma_\beta^2}\right)\right] \times \exp\left[-\frac{(\mathbf{r}_1 - \mathbf{r}_2)^2}{2\delta_{\alpha\beta}^2}\right], \quad (\alpha, \beta) \in (x, y), \tag{33}$$

where A_α and σ_α characterize the peak value and the width of the spectral density of the α component, respectively, while $\delta_{\alpha\beta}$ and (complex) $B_{\alpha\beta}$ represent the transverse extent and single-point value of the field correlations between the α and β components. From the properties of the CSD matrix, it follows that $B_{xx} = B_{yy} = 1$, $\delta_{xy} = \delta_{yx}$, and $B_{xy} = B_{yx}^*$, with $|B_{xy}| \leqslant 1$. Moreover, for a realizable GSM source it is required that $\max(\delta_{xx}, \delta_{yy}) \leqslant \delta_{xy} \leqslant \min(\delta_{xx}/\sqrt{|B_{xy}|}, \delta_{yy}/\sqrt{|B_{xy}|})$ [7]. All listed parameters are independent of position but may depend on frequency.

1. *Rotationally symmetric GSM beam*

We first assess the special class of rotationally symmetric, uniformly partially polarized GSM beams [21] for which we set $A_x = A_y = A$, $\sigma_x = \sigma_y = \sigma$, and $\delta_{xx} = \delta_{yy} = \delta_{xy} = \delta$. The CSD matrix can therefore be written as

$$\mathbf{W}_{12} = A^2\exp\left(-\frac{\mathbf{r}_1^2 + \mathbf{r}_2^2}{2\sigma^2}\right)\exp\left(-\frac{|\Delta\mathbf{r}|^2}{2\delta^2}\right) \times \begin{bmatrix} 1 & B_{xy} \\ B_{xy}^* & 1 \end{bmatrix}, \tag{34}$$

where we introduced $\Delta\mathbf{r} = \mathbf{r}_2 - \mathbf{r}_1$. Inserting $\mathbf{r}_1 = \mathbf{r}_2 = \mathbf{r}$ results in the polarization matrix

$$\boldsymbol{\Phi} = A^2\exp\left(-\frac{\mathbf{r}^2}{\sigma^2}\right)\begin{bmatrix} 1 & B_{xy} \\ B_{xy}^* & 1 \end{bmatrix}, \tag{35}$$

whose unpolarized and polarized parts read, respectively,

$$\boldsymbol{\Phi}^{(\mathrm{u})} = A^2\exp\left(-\frac{\mathbf{r}^2}{\sigma^2}\right)\begin{bmatrix} 1-P & 0 \\ 0 & 1-P \end{bmatrix}, \tag{36}$$

$$\boldsymbol{\Phi}^{(\mathrm{p})} = A^2\exp\left(-\frac{\mathbf{r}^2}{\sigma^2}\right)\begin{bmatrix} P & B_{xy} \\ B_{xy}^* & P \end{bmatrix}, \tag{37}$$

where we used the fact that for the polarized constituent $\det \boldsymbol{\Phi}^{(\mathrm{p})} = 0$ and thus $|B_{xy}| = P$, with P denoting the degree of polarization given in Eq. (3). Further, using Eqs. (7) and (34), the Gram matrix is found and has the form

$$\boldsymbol{\Omega}_{12} = A^4 \exp\left(-\frac{\mathbf{r}_1^2 + \mathbf{r}_2^2}{\sigma^2}\right)\exp\left(-\frac{|\Delta\mathbf{r}|^2}{\delta^2}\right) \times \begin{bmatrix} 1+P^2 & 2B_{xy} \\ 2B_{xy}^* & 1+P^2 \end{bmatrix}. \quad (38)$$

Equation (12) implies

$$P_\Omega(\mathbf{r}_1, \mathbf{r}_2) = \frac{2P}{1+P^2}. \quad (39)$$

The normalized Stokes parameters defined in Eq. (18) are

$$q_0 = \exp\left(-\frac{|\Delta\mathbf{r}|^2}{\delta^2}\right)\frac{1+P^2}{2} = \mu^2, \quad (40a)$$

$$q_1 = 0, \quad (40b)$$

$$q_2 = \exp\left(-\frac{|\Delta\mathbf{r}|^2}{\delta^2}\right)\mathrm{Re}(B_{xy}), \quad (40c)$$

$$q_3 = \exp\left(-\frac{|\Delta\mathbf{r}|^2}{\delta^2}\right)\mathrm{Im}(B_{xy}). \quad (40d)$$

The coherence Poincaré vector $\mathbf{q} = \mathbf{q}_{12} = \mathbf{q}_{21}$ can be written as

$$\mathbf{q} = P \exp\left(-\frac{|\Delta\mathbf{r}|^2}{\delta^2}\right)\hat{\mathbf{s}}, \quad (41)$$

where

$$\hat{\mathbf{s}} = [0, \cos[\arg(B_{xy})], \sin[\arg(B_{xy})]] \quad (42)$$

is the (unit) polarization Poincaré vector of the fully polarized part of the field with the polarization matrix given in Eq. (37). The $\mathbf{q}$ vector for the chosen symmetric GSM beam lies in the q_2q_3 plane on a circle whose radius is determined by the degree of polarization together with the factor $\exp(-|\Delta\mathbf{r}|^2/\delta^2)$, which reflects the degree of coherence. The direction of $\mathbf{q}$ is specified by the polarization Poincaré vector $\hat{\mathbf{s}}$ of the fully polarized beam portion. We further observe that the surface of the (unit) sphere is approached when $P = 1$ and $|\Delta\mathbf{r}| \to 0$, whereas the origin is reached when $P = 0$ or $|\Delta\mathbf{r}| \to \infty$.

2. Rotationally nonsymmetric GSM beam

Next, we consider a uniformly partially polarized GSM beam with rotationally nonsymmetric coherence properties. For this purpose we set $\delta_{xx} = \delta$, $\delta_{yy} = a\delta$, and $\delta_{xy} = b\delta$, with restrictions set by the realizability conditions [see discussion below Eq. (33)]. The CSD matrix of such a beam is written as

$$\mathbf{W}_{12} = A^2 \exp\left(-\frac{\mathbf{r}_1^2 + \mathbf{r}_2^2}{2\sigma^2}\right)\begin{bmatrix} \Theta & B_{xy}\Theta^{1/b^2} \\ B_{xy}^*\Theta^{1/b^2} & \Theta^{1/a^2} \end{bmatrix}, \quad (43)$$

where $\Theta = \exp[-|\Delta\mathbf{r}|^2/(2\delta^2)]$, for brevity. With a procedure similar to the one that led to Eqs. (40a)–(40d), the normalized Stokes parameters are found to be

$$q_0 = \tfrac{1}{4}\left(\Theta^2 + \Theta^{2/a^2} + 2\Theta^{2/b^2}P^2\right) = \mu^2, \quad (44a)$$

$$q_1 = \tfrac{1}{4}\left(\Theta^2 - \Theta^{2/a^2}\right), \quad (44b)$$

$$q_2 = \tfrac{1}{2}\left[\Theta^{1/b^2}\left(\Theta + \Theta^{1/a^2}\right)\mathrm{Re}(B_{xy})\right], \quad (44c)$$

$$q_3 = \tfrac{1}{2}\left[\Theta^{1/b^2}\left(\Theta + \Theta^{1/a^2}\right)\mathrm{Im}(B_{xy})\right], \quad (44d)$$

and

$$\mathbf{q} = \tfrac{1}{4}\left(\Theta^2 - \Theta^{2/a^2}, 0, 0\right) + \tfrac{1}{2}\Theta^{1/b^2}\left(\Theta + \Theta^{1/a^2}\right)P\hat{\mathbf{s}}, \quad (45)$$

where again $\hat{\mathbf{s}}$ is the polarization Poincaré vector of the beam's fully polarized constituent as presented in Eq. (42). The coherence Poincaré vector depends on the two spatial points only through their separation $|\Delta\mathbf{r}|$. As seen from Eq. (45), the coherence Poincaré vector can be divided into two parts, the first of which points along the q_1 axis with the length determined by $\Theta^2 - \Theta^{2/a^2}$. Besides the distance $|\Delta\mathbf{r}|$, it depends only on the coherence-width ratio $a = \delta_{yy}/\delta_{xx}$ of the beam. The second vector is located in the q_2q_3 plane, and its direction is determined solely by the polarization Poincaré vector $\hat{\mathbf{s}}$ of the beam's fully polarized part, while its length is influenced by the degree of polarization and coherence-width ratios a and $b = \delta_{xy}/\delta_{xx}$. In other words, the beam's polarization properties affect the geography of the coherence Poincaré vector on only the q_2q_3 plane, whereas the displacement along the q_1 axis is dictated by the ratio of the coherence widths in the x and y directions via a. We can also state that if the two-point coherence properties are kept fixed but the polarization state is varied, the $\mathbf{q}$ vector traces a circle with its center at the q_1 axis. The direction of $\mathbf{q}$ with respect to the center point (corresponding to an unpolarized beam) is determined by the state of polarization. If $a = 1$, the first vector (asymmetry) in Eq. (45) disappears, and $\mathbf{q}$ is located on a sphere in the q_2q_3 plane for any b, P, and $\hat{\mathbf{s}}$. Moreover, if also $b = 1$, the case reduces to the rotationally symmetric GSM beams encountered in Eq. (41). In conclusion, we state that an asymmetry of the coherence lengths in the x and y directions induces a displacement of the vector $\mathbf{q}$ along the q_1 axis.

3. Anisotropic GSM beams

In the final example we consider a class of anisotropic GSM beams for which $\sigma_x \neq \sigma_y$. As in the first GSM example, we assume symmetry in the coherence widths, $\delta_{xx} = \delta_{yy} = \delta_{xy} = \delta$, and mark $A_x = A_y = A$. With these selections we revisit Eq. (33) and arrive at the CSD matrix

$$\mathbf{W}_{12} = A^2 \exp\left(-\frac{|\Delta\mathbf{r}|^2}{2\delta^2}\right) \times \begin{bmatrix} \Delta_{xx}(\mathbf{r}_1, \mathbf{r}_2) & B_{xy}\Delta_{xy}(\mathbf{r}_1, \mathbf{r}_2) \\ B_{xy}^*\Delta_{yx}(\mathbf{r}_1, \mathbf{r}_2) & \Delta_{yy}(\mathbf{r}_1, \mathbf{r}_2) \end{bmatrix}, \quad (46)$$

where

$$\Delta_{\alpha\beta}(\mathbf{r}_1, \mathbf{r}_2) = \exp\left[-\left(\frac{\mathbf{r}_1^2}{2\sigma_\alpha^2} + \frac{\mathbf{r}_2^2}{2\sigma_\beta^2}\right)\right]. \quad (47)$$

We follow anew the steps that preceded Eqs. (41) and (45) and obtain the expressions

$$\mathbf{q}_{12} = \exp\left(-\frac{|\Delta\mathbf{r}|^2}{\delta^2}\right) \times \begin{bmatrix} \frac{\Delta_{xx}^2(\mathbf{r}_1,\mathbf{r}_2)-\Delta_{yy}^2(\mathbf{r}_1,\mathbf{r}_2)+|B_{xy}|^2[\Delta_{yx}^2(\mathbf{r}_1,\mathbf{r}_2)-\Delta_{xy}^2(\mathbf{r}_1,\mathbf{r}_2)]}{\Delta_{xx}^2(\mathbf{r}_1,\mathbf{r}_2)+\Delta_{yy}^2(\mathbf{r}_1,\mathbf{r}_2)+\Delta_{yx}^2(\mathbf{r}_1,\mathbf{r}_2)+\Delta_{xy}^2(\mathbf{r}_1,\mathbf{r}_2)} \\ \frac{2\mathrm{Re}(B_{xy})\Delta_{xy}^2(\mathbf{r}_2,\mathbf{r}_2)[\Delta_{xx}^2(\mathbf{r}_1,\mathbf{r}_1)+\Delta_{yy}^2(\mathbf{r}_1,\mathbf{r}_1)]}{\Delta_{xx}^2(\mathbf{r}_1,\mathbf{r}_2)+\Delta_{yy}^2(\mathbf{r}_1,\mathbf{r}_2)+\Delta_{yx}^2(\mathbf{r}_1,\mathbf{r}_2)+\Delta_{xy}^2(\mathbf{r}_1,\mathbf{r}_2)} \\ \frac{2\mathrm{Im}(B_{xy})\Delta_{xy}^2(\mathbf{r}_2,\mathbf{r}_2)[\Delta_{xx}^2(\mathbf{r}_1,\mathbf{r}_1)+\Delta_{yy}^2(\mathbf{r}_1,\mathbf{r}_1)]}{\Delta_{xx}^2(\mathbf{r}_1,\mathbf{r}_2)+\Delta_{yy}^2(\mathbf{r}_1,\mathbf{r}_2)+\Delta_{yx}^2(\mathbf{r}_1,\mathbf{r}_2)+\Delta_{xy}^2(\mathbf{r}_1,\mathbf{r}_2)} \end{bmatrix}^{\mathrm{T}}, \quad (48)$$

$$\mathbf{q}_{21} = \exp\left(-\frac{|\Delta\mathbf{r}|^2}{\delta^2}\right) \times \begin{bmatrix} \frac{\Delta_{xx}^2(\mathbf{r}_1,\mathbf{r}_2)-\Delta_{yy}^2(\mathbf{r}_1,\mathbf{r}_2)+|B_{xy}|^2[\Delta_{xy}^2(\mathbf{r}_1,\mathbf{r}_2)-\Delta_{yx}^2(\mathbf{r}_1,\mathbf{r}_2)]}{\Delta_{xx}^2(\mathbf{r}_1,\mathbf{r}_2)+\Delta_{yy}^2(\mathbf{r}_1,\mathbf{r}_2)+\Delta_{yx}^2(\mathbf{r}_1,\mathbf{r}_2)+\Delta_{xy}^2(\mathbf{r}_1,\mathbf{r}_2)} \\ \frac{2\mathrm{Re}(B_{xy})\Delta_{xy}^2(\mathbf{r}_1,\mathbf{r}_1)[\Delta_{xx}^2(\mathbf{r}_2,\mathbf{r}_2)+\Delta_{yy}^2(\mathbf{r}_2,\mathbf{r}_2)]}{\Delta_{xx}^2(\mathbf{r}_1,\mathbf{r}_2)+\Delta_{yy}^2(\mathbf{r}_1,\mathbf{r}_2)+\Delta_{yx}^2(\mathbf{r}_1,\mathbf{r}_2)+\Delta_{xy}^2(\mathbf{r}_1,\mathbf{r}_2)} \\ \frac{2\mathrm{Im}(B_{xy})\Delta_{xy}^2(\mathbf{r}_1,\mathbf{r}_1)[\Delta_{xx}^2(\mathbf{r}_2,\mathbf{r}_2)+\Delta_{yy}^2(\mathbf{r}_2,\mathbf{r}_2)]}{\Delta_{xx}^2(\mathbf{r}_1,\mathbf{r}_2)+\Delta_{yy}^2(\mathbf{r}_1,\mathbf{r}_2)+\Delta_{yx}^2(\mathbf{r}_1,\mathbf{r}_2)+\Delta_{xy}^2(\mathbf{r}_1,\mathbf{r}_2)} \end{bmatrix}^{\mathrm{T}} \quad (49)$$

for $\mathbf{q}_{12}$ and $\mathbf{q}_{21}$. While the two previously considered classes of GSM beams could be expressed in terms of a single coherence Poincaré vector, this example shows the situation for $\mathbf{q}_{12} \neq \mathbf{q}_{21}$. In this case the difference in the two coherence Poincaré vectors naturally arises from the assumed difference between σ_x and σ_y. The connection between the two coherence vectors and the polarization state is now more involved than in the previous examples. Nonetheless, they describe the state of the two singular vectors related to the largest singular value of the CSD. Figure 2 displays the behavior of $\mathbf{q}_{12}$ (red arrows) and $\mathbf{q}_{21}$ (blue arrows) on the coherence Poincaré sphere as a function of the ratio σ_y/σ_x for the beam parameters $\delta_{xx} = \delta_{yy} = \delta_{xy} = 0.1\sigma_x$ and $|B_{xy}| = 0.95$. The cases A, B, and C correspond to the values of $\arg(B_{xy}) = \pi/2$, $\arg(B_{xy}) = 0$, and $\arg(B_{xy}) = 3\pi/2$ at two points $\mathbf{r}_1 = (0.1\sigma_x, 0)$, $\mathbf{r}_2 = (0.15\sigma_x, 0)$. The arrows indicate the case of $\sigma_y/\sigma_x = 0.1$, and the corresponding dashed lines represent the path that the vector tips draw as the width ratio increases. When the ratio attains unity, the green vector referring to $\mathbf{q}_{12} = \mathbf{q}_{21}$ is obtained, and the situation reduces to the case of a rotationally symmetric GSM beam. This is confirmed also in Fig. 3, where the change in the central angle θ_{12} defined in Eq. (28) is shown as a function of σ_y/σ_x with other beam parameters corresponding to case C of Fig. 2. The evolution of θ_{12} shows at once the geometric similarity between the coherence states of $\mathbf{q}_{12}$ and $\mathbf{q}_{21}$. The coherence information in the two vectors is the same when σ_y is close to zero or equal to its orthogonal counterpart, $\sigma_y = \sigma_x$.

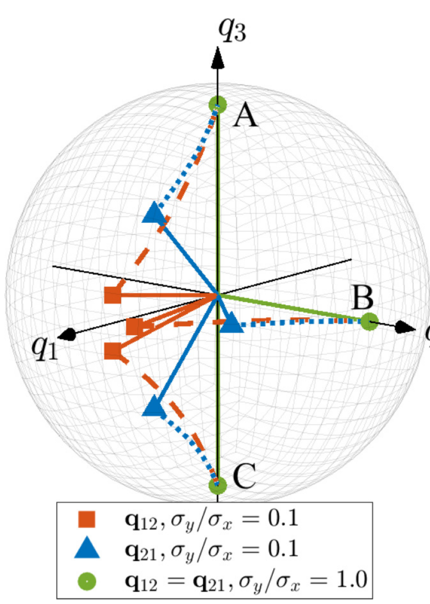

FIG. 2. Behavior of the coherence Poincaré vectors with respect to the intensity width ratio σ_y/σ_x of anisotropic GSM beams for $\mathbf{r}_1 = (0.1\sigma_x, 0)$, $\mathbf{r}_2 = (0.15\sigma_x, 0)$, $\delta_{xx} = \delta_{yy} = \delta_{xy} = 0.1\sigma_x$, $|B_{xy}| = 0.95$, and $\arg(B_{xy}) = \pi/2$ (A), $\arg(B_{xy}) = 0$ (B), and $\arg(B_{xy}) = 3\pi/2$ (C). Starting from $\sigma_y/\sigma_x = 0.1$, the beam's coherence state is displayed by two vectors $\mathbf{q}_{12}$ (red square head) and $\mathbf{q}_{21}$ (blue triangle head) which point at separate directions. The red dashed line and the blue dotted line show the change in these directions as the intensity ratio approaches a value of unity. When $\sigma_x = \sigma_y$, the beam is a rotationally symmetric GSM beam, and a single vector $\mathbf{q}_{12} = \mathbf{q}_{21}$ (green circle head) shows the situation within the coherence Poincaré sphere.

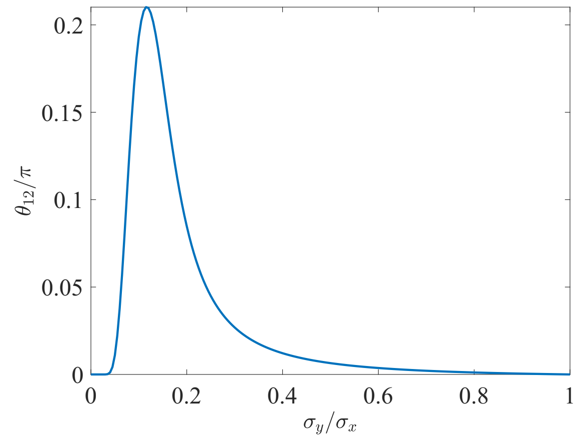

FIG. 3. Evolution of the normalized central angle θ_{12}/π with respect to the intensity width ratio σ_y/σ_x of anisotropic GSM beams. The value $\arg(B_{xy}) = 3\pi/2$ was used, and the other parameters are as in Fig. 2.

V. CONCLUSIONS

In conclusion, we established a rigorous interpretation for the coherence Poincaré sphere construction in the context of partially nonuniformly polarized electromagnetic beams in the space-frequency domain. This work can be viewed as an extension of the formalism in [10] to cover general partially polarized light beams. The main result is that in the context of partial polarization, two coherence Poincaré vectors are needed whose directions are specified by the state of spatial coherence via the singular vectors related to the larger singular value of the CSD matrix. The two vectors have the same length, which equals unity for fully coherent beams and zero for completely incoherent beams or fields which are purely unpolarized (or can be transformed into this type by unitary transformations at two points). In the case of full polarization the formalism of [10] is encountered, and when the two points coincide, the traditional polarization Poincaré formalism is recovered. In addition, we demonstrated the sphere representation of spatial coherence with examples including paraxial blackbody radiation as well as GSM beams.

The results of this work may find use in visualizing the coherence-polarization state of light in various situations involving partially polarized beams. These might include the polarization and coherence changes induced by, e.g., the scattering of electromagnetic plane waves from localized objects [22], beam propagation in turbulence [23] or through ABCD systems such as optical fibers [24], free-space propagation of beams from nonuniformly correlated [25] or multi-Gaussian Schell-model [26] sources, and twisted beams with rotating polarization properties [27].

ACKNOWLEDGMENTS

This work was supported by the Academy of Finland [Projects No. 308393, No. 310511, and No. 320166 (PREIN)]. O.K. thanks the Joensuu University Foundation for financial support.

[1] M. Born and E. Wolf, *Principles of Optics*, 7th ed. (Cambridge University Press, Cambridge, 1999).
[2] L. Mandel and E. Wolf, *Optical Coherence and Quantum Optics* (Cambridge University Press, Cambridge, 1995).
[3] O. Korotkova and G. Gbur, Applications of optical coherence theory, in *Progress in Optics*, edited by T. D. Visser (Elsevier, Amsterdam, 2020), Vol. 65, pp. 43–104.
[4] C. Brosseau, *Fundamentals of Polarized Light: A Statistical Optics Approach* (Wiley, New York, 1998).
[5] E. Wolf, *Introduction to the Theory of Coherence and Polarization of Light* (Cambridge University Press, Cambridge, 2007).
[6] R. Martínez-Herrero, P. M. Mejías, and G. Piquero, *Characterization of Partially Polarized Light Fields* (Springer, Berlin, 2009).
[7] O. Korotkova, *Random Light Beams: Theory and Applications* (CRC Press, Boca Raton, FL, 2014).
[8] J. J. Gil and R. Ossikovski, *Polarized Light and the Mueller Matrix Approach* (CRC Press, Boca Raton, FL, 2016).
[9] A. T. Friberg and T. Setälä, Electromagnetic theory of optical coherence [Invited], J. Opt. Soc. Am. A **33**, 2431 (2016).
[10] J. Laatikainen, A. T. Friberg, O. Korotkova, and T. Setälä, Poincaré sphere of electromagnetic spatial coherence, Opt. Lett. **46**, 2143 (2021).
[11] A. Nielsen and I. L. Chuang, *Quantum Computation and Quantum Information* (Cambridge University Press, Cambridge, 2010).
[12] J. Tervo, T. Setälä, and A. T. Friberg, Theory of partially coherent electromagnetic fields in the space–frequency domain, J. Opt. Soc. Am. A **21**, 2205 (2004).
[13] J. Tervo, T. Setälä, and A. T. Friberg, Degree of coherence for electromagnetic fields, Opt. Express **11**, 1137 (2003).
[14] T. Setälä, J. Tervo, and A. T. Friberg, Contrasts of Stokes parameters in Young's interference experiment and electromagnetic degree of coherence, Opt. Lett. **31**, 2669 (2006)
[15] L. P. Kuptsov, in *Encyclopedia of Mathematics*, edited by M. Hazewinkel (Kluwer, Dordrecht, 1989), Vol. 4, p. 293.
[16] G. W. Stewart, *Matrix Algorithms: Basic Decompositions* (Society for Industrial and Applied Mathematics, Philadelphia, 1998).
[17] P. Réfrégier and A. Roueff, Intrinsic degrees of coherence for electromagnetic fields, in *Advances in Information Optics and Photonics*, edited by A. T. Friberg and R. Dändliker (SPIE, Bellingham, WA, 2008), Chap. 10, pp. 189–209.
[18] F. Gori, J. Tervo, and J. Turunen, Correlation matrices of completely unpolarized beams, Opt. Lett. **34**, 1447 (2009).
[19] M. Lahiri and E. Wolf, Cross-spectral density matrix of the far field generated by a blackbody source, Opt. Commun. **281**, 3241 (2008).
[20] K. Blomstedt, A. T. Friberg, and T. Setälä, Classical coherence of blackbody radiation, Prog. Opt. **62**, 293 (2017).
[21] L.-P. Leppänen, A. T. Friberg, and T. Setälä, Connection of electromagnetic degrees of coherence in space–time and space–frequency domains, Opt. Lett. **41**, 1821 (2016).
[22] Z. Tong and O. Korotkova, Theory of weak scattering of stochastic electromagnetic fields from deterministic and random media, Phys. Rev. A **82**, 033836 (2010).
[23] O. Korotkova, M. Salem, and E. Wolf, The far-zone behavior of the degree of polarization of partially coherent beams propagating through atmospheric turbulence, Opt. Commun. **233**, 225 (2004).
[24] H. Roychowdhury, G. P. Agrawal, and E. Wolf, Changes in the spectrum, in the spectral degree of polarization, and in the spectral degree of coherence of a partially coherent beam propagating through a gradient-index fiber, J. Opt. Soc. Am. A **23**, 940 (2006).
[25] Z. Tong and O. Korotkova, Electromagnetic nonuniformly correlated beams, J. Opt. Soc. Am. A **29**, 2154 (2012).
[26] Z. Mei, O. Korotkova, and E. Shchepakina, Electromagnetic multi-Gaussian Schell-model beams, J. Opt. **15**, 025705 (2013).
[27] Z. Mei and O. Korotkova, Twisted EM beams with structured correlations, Opt. Lett. **43**, 3905 (2018).